Simplified Power Consumption Modeling and Identification for Wheeled Skid-Steer Robotic Vehicles on Hard Horizontal Ground

Jesús Morales, Jorge L. Martínez, Anthony Mandow, Alejandro Pequeño-Boter, and Alfonso García-Cerezo
Dpto. Ingeniería de Sistemas y Automática, Universidad de Málaga, 29071 Málaga, Spain
Email: jesus.morales@uma.es, Tel: (+34) 951 952323

Abstract— **Autonomous mobile robots have limited energy sources. This work studies power consumption of the locomotion system of wheeled skid-steer vehicles on hard horizontal terrain at walking speeds. This issue is very important for this kind of vehicles due to relevant power losses associated to dynamic friction during turnings. The paper adopts a kinematics approach to provide a simplified power model. This static model estimates motor power consumption as a function of the left- and right-side wheels' speeds. The model is defined through three constant parameters: the x-coordinate of the treads' instantaneous center of rotation on the ground plane, a traction resistance constant, and the ground-wheel friction coefficient. Furthermore, a simple experimental identification procedure is proposed to obtain the model parameters. A power analysis of the four-wheel skid-steer mobile robot Quadriga has been performed with different loads on concrete and marble floorings.**

I. INTRODUCTION

Wheeled skid-steering is based on controlling the relative velocities of the left and right side drives, similarly to differential drive vehicles. However, since all wheels are aligned with the longitudinal axis of the vehicle, turning requires wheel slippage. Wheeled skid-steering presents two major advantages over alternative wheel configurations, such as Ackermann or axle-articulated. First, it is simple and robust, as it uses only the mechanical components needed for straight line motion. Second, it provides better maneuverability, including zero-radius turning [1].

This locomotion system is found in heavy vehicles for agriculture [2], construction, and military operations [3] [4], and also in much lighter mobile robots [5]. Field applications of wheeled skid-steer unmanned ground vehicles include planetary exploration [1], reconnaissance of dangerous areas [6], and search & rescue [7], which require a high degree of autonomy with limited power sources.

In this kind of robotic vehicles, power consumption is very important due to relevant power losses associated to dynamic friction during turnings [8]. To reduce these losses, active wheel suspension can be applied when turning [9].

A power consumption model can be very valuable for effective autonomous mission planning and execution. For example, it can be used to predict when the vehicle needs to be recharged, to find out whether a given task can be completed with the available energy, or to ascertain if motors can provide sufficient power to follow a trajectory (i.e., speed and curvature) on a given terrain.

A power model based on a dynamic analysis has been recently presented for a commercial research platform [10]. However, this model does not consider turning on spot, which is the most power demanding case. A comprehensive static model for skid power consumption was proposed in [11] for tracked vehicles.

This paper proposes a static power consumption model for wheeled skid-steering robotic vehicles. This model, which is a development from [11], is based on approximate wheeled skid-steer kinematics [12]. The simplified model, which is defined by three constant parameters, relates motor power consumption with the left- and right-side wheels' speeds. Furthermore, the paper offers an easy experimental procedure to obtain the model parameters. This method has been applied to the case study of the Quadriga mobile robot with different loads on concrete and marble floorings.

Following this introduction, section 2 reviews kinematics for wheeled skid-steer mobile robots. Section 3 states a simplified power consumption model for this kind of vehicles and proposes an experimental procedure for parameter identification. Section 4 analyzes results from the Quadriga mobile robot case-study. Section 5 is devoted to conclusions and ideas for future work. Finally, acknowledgements and references complete the paper.

II. KINEMATIC APPROXIMATION

This section briefly reviews the work presented in [12], where approximate kinematics for wheeled skid-steer vehicles is obtained as a function of the Instantaneous Centers of Rotation (ICRs) of the left and right side wheel treads on the 2D ground plane. These tread ICRs, which are different from the vehicle's single ICR, represent the positions of a pair of equivalent differential drive ideal wheel contact points, as illustrated by Fig. 1.

Let us assume that the local frame of the vehicle has its origin in the geometrical center of the convex area spanned by the wheels' contact points and its Y axis is aligned with the forward motion direction (see Fig. 1). The XY plane is defined to be parallel to the ground plane.

Local vectors can be defined as $\vec{C}^l$ and $\vec{C}^r$ for the left and right tread ICRs, respectively. Their coordinates are $\vec{C}^{l,r} = (C_x^{l,r}, C_y, 0)$, where l, r denotes any of both treads. Both ICRs have the same Y coordinate C_y since they lie beyond their corresponding tread centerlines on a line that is parallel to the local X axis.
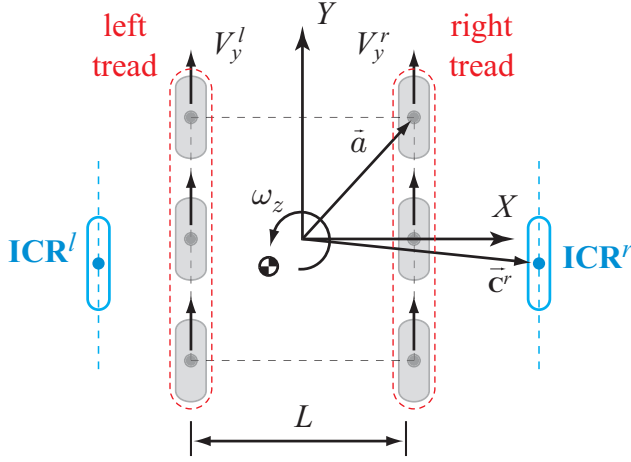
Fig. 1. Tread ICRs on the motion plane represented as virtual wheels.

The local coordinates of tread ICRs are dynamics-dependent. Nevertheless, they remain within a bounded area. When the vehicle moves at walking speeds, optimized constant values for tread ICR positions can be obtained from experimental identification [12].

Tread ICR positions depend on terrain type and vehicle design, especially on the position of the center of gravity and on the wheel type. Tire pressure also affects tread ICR coordinates.

With this kinematic approximation, the angular speed of the vehicle ω_z can be calculated as:

$$\omega_z = \frac{V_y^r - V_y^l}{C_x^r - C_x^l}, \tag{1}$$

where V_y^l and V_y^r are the longitudinal speeds for the left and right side wheels, respectively.

III. MOTOR POWER CONSUMPTION MODELING AND IDENTIFICATION

A. Simplified Power Consumption Model

Using a derivation similar to [11] and assuming a punctual contact point for each wheel, the power lost due to slippage P_S can be approximately modeled as:

$$\hat{P}_S = \mu \left|\omega_z\right| \sum_{\forall a^{l,r}} \left(p(a^{l,r}) \| \vec{a}^{l,r} - \vec{C}^{l,r} \| \right), \tag{2}$$

where μ is the friction coefficient, a represents the contact point of a wheel, $\vec{a}$ is the coordinate vector of a relative to the local frame, and $p(a)$ is the pressure under each contact point a.

Apart from dynamic friction, the motors have to provide power for other traction resistances. These include frictions caused by the deformation of the wheels and soil-shearing, and internal frictions of the transmission belts and the gearheads. At walking speeds, the power drawn due to these factors P_R can be modeled approximately as proportional to the absolute value of the tread speeds, as follows:

$$\hat{P}_R = K \left(|V_y^l| + |V_y^r|\right), \tag{3}$$

where K denotes the proportional traction resistance constant [11].

Therefore, the total mechanical power provided by the motors P_M can be estimated as the sum of (2) and (3):

$$\hat{P}_M = \hat{P}_S + \hat{P}_R. \tag{4}$$

B. Experimental Identification

To obtain a simplified motor power consumption model for a wheeled skid-steer mobile robot on flat hard terrain at walking speeds, the following experimental procedure can be performed.

First, it is necessary to identify local coordinates of the tread ICRs. In most cases, it suffices to consider symmetric tread ICRs, where $C_x^r = -C_x^l = C_x$ and $C_y = 0$. Coordinate C_x can be estimated by measuring the total rotated angle ϕ when equal opposite speeds are applied to both treads [12]:

$$\hat{C}_x = \frac{\int V \, dt}{\phi}, \tag{5}$$

where $V = V_y^r = -V_y^l$.

Second, the local coordinates of the contact points of the wheels on the ground $\vec{a}$ have to be determined. Also, the punctual pressure under these points $p(a)$ has to be measured in force units.

Third, a representative path has to be executed to obtain identification data. Especially, spiral-like paths can be of interest because they offer a comprehensive combination of wheel speeds, from straight line motion to turning on spot. In particular, the following data should be collected:

- The longitudinal speeds of the left and right side wheels: $V_y^{l,r}$.
- The total mechanical power delivered by the motors: P_M.

Finally, experimental data is used to optimally adjust parameters K and μ by evaluating (4) and comparing it with the measured value of P_M.

IV. CASE STUDY: APPLICATION TO QUADRIGA

Quadriga is a 4-wheel skid-steer mobile robot (see Fig. 2). Its dimensions are 0.82 m length, 0.64 m width, 0.47 m height. The vehicle weights 83.1 kg when carrying an empty 64 l water tank, and its payload is 90 kg. The distance between the front and rear wheel contact points is 0.475 m. The wheels are pneumatic tires of 35.5 cm diameter and have rigid suspension. Distance between left and right wheel contact points is $L = 0.5$ m. Quadriga has a maximum linear speed of 1.2 m/s.

A scheme of Quadriga's drive system is shown in Fig. 3. This system uses two permanent magnet DC motors, equipped with gearheads and optical quadrature shaft encoders. Wheels at each side are mechanically coupled by a chain transmission. Motors are controlled by an embedded board that integrates a microcontroller (μC) and two independent H-bridge power stages. Power is supplied by a 36 V battery pack, which is composed of six 12 V lead-acid batteries connected in a series-parallel configuration.

Fig. 2. The Quadriga mobile robot on marble flooring with a water tank.

A. Experimental Power Model

The experimental model has been estimated on two terrain types: marble flooring and concrete, and with the water tank full and empty.

The first step in the power model identification procedure is estimating the local x-coordinate of the tread ICRs. Applying (5) with data from turning on spot experiments has given the same $\hat{C}_x = 0.47\,\mathrm{m}$ for the four terrain-load combinations.

The pressure under each wheel has been measured with four scales for the full and empty water tank cases (see Fig. 4). In both cases, the center of gravity is almost coincident with the origin of the local frame of the vehicle (see Table I). This fact supports the assumption of symmetric tread ICRs [13].

TABLE I

LOCAL COORDINATES OF THE CENTER OF GRAVITY FOR THE FULL AND EMPTY TANK CASES.

	Full	Empty
x (cm)	0.05	−0.06
y (cm)	2.02	0.89

The motor power stages employed in this vehicle are regenerative, which means that most electric power can be transferred back to the batteries a motor acts as a generator (i.e., motor power consumption is negative [11]).

Hall Effect current sensors have been installed to measure the instantaneous power consumption of each motor P_M^l, P_M^r. With this configuration, measurements are not affected by the consumption of other vehicle components unrelated to the traction system. Thus, the total mechanical power of the traction system P_M can be calculated as:

$$P_M = P_M^l + P_M^r. \tag{6}$$

Data acquisition and high level motion control are performed by a compact onboard computer using a LabVIEW program. This computer interfaces with the embedded motor controller and the current sensors through two serial links. Manual operation is possible through a wireless joystick.

The summation in (2) is a constant value if constant tread ICR positions are assumed. For Quadriga, this constant is $466\,\mathrm{Nm}$ and $264\,\mathrm{Nm}$ for the full and empty tank cases, respectively.

With data acquired from a manually guided spiral-like path, parameters K and μ can be easily identified by using the Simplex optimization method [14]. The cost function to be minimized is based on the error between (4) and (6):

$$J(K, \mu) = \sum_{\forall t} |\hat{P}_M(t;\, K,\, \mu) - P_M(t)|. \tag{7}$$

Figure 5 presents measurements from the experiment on marble flooring with the full tank. Note that in the interval from $7\,\mathrm{s}$ to $17\,\mathrm{s}$, the left and right side wheels move forward but with different speeds. This provokes that the right side wheels are dragged by the faster left side [11]. Therefore, the right motor is acting as a generator as shown by its negative P_M^r values. This does not happen when wheel speeds are similar or have opposite signs.

Fig. 3. Drive system scheme of Quadriga mobile robot.
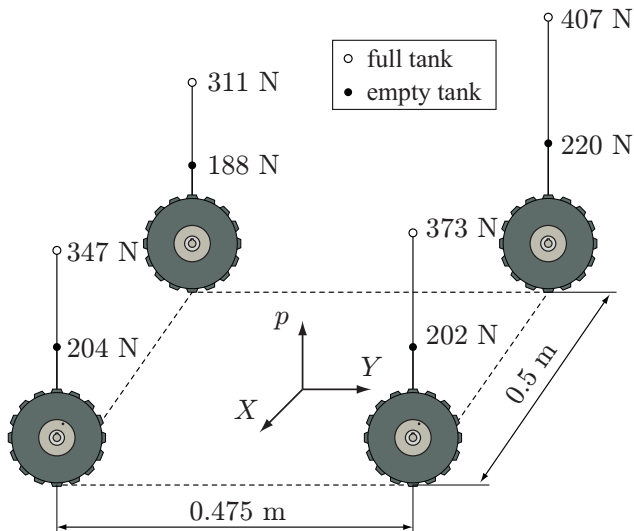
Fig. 4. Punctual pressure distribution under each wheel with the water tank empty and full.
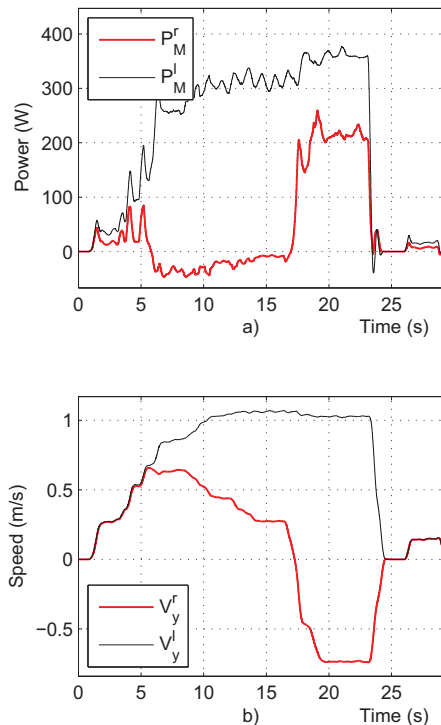
Fig. 5. Experimental data from manually guided spiral-like path with marble flooring and full tank: a) Motor power consumption, and b) wheel speeds.

Table II shows the resulting parameters for the four case study combinations. As for the friction coefficient μ, estimations corroborate that it only depends on terrain type, with a higher value for concrete. The value of K is slightly affected by load and terrain type. With the hoisted vehicle, the estimation of this parameter renders $59\,\mathrm{N}$, which reveals that internal frictions are a very relevant component of the traction resistance.

$K - \mu$	Full	Empty
Marble	$110\,\mathrm{N} - 0.431$	$90\,\mathrm{N} - 0.427$
Concrete	$118\,\mathrm{N} - 0.647$	$113\,\mathrm{N} - 0.627$

B. Experimental validation

A manually driven 8-shaped path has been considered for experimental validation of the four case-study models. A comparison between the measured and model-based values of P_M is offered in Figs. 6–9 for the corresponding four paths. The inputs of the model, i.e., the left- and right-side wheel speeds, are also shown.

In general, even if the model does not reproduce high frequency power consumption variations, the model-based estimations closely resemble the measured values for all the wheel speed combinations in the validation paths. As this is a static model, the highest estimation errors occur in instants when motors have high acceleration values (e.g., around $33\,\mathrm{s}$ in Fig. 6).

The figures also present a comparison of the integrals of actual and estimated power consumption (i.e., energy consumption during each experiment). Note that the high frequency variations have no visible effect on energy estimations. With the exception of errors due to high accelerations, the energy estimation offered by the simplified model is quite accurate.

V. CONCLUSIONS

Power consumption is a very important issue for skid-steer robotic vehicles due to relevant power losses associated to dynamic friction during turning. This work has proposed a simplified power consumption model for wheeled skid-steer robotic vehicles on hard horizontal ground at walking speeds based on a kinematics approach. This static model provides an estimation of motor power consumption as a function of the left- and right-side wheels' speeds. The model is defined through three parameters: the x-coordinate of the treads' ICR, a traction resistance constant, and the ground-wheel friction coefficient.

A simple experimental procedure has been proposed to identify the three model parameters. First, a turn-on-spot experiment can be used to estimate the treads' ICR. Then, data from a simple spiral-like path is fed to an optimization method to obtain the traction resistance constant and the friction coefficient.

This model and the identification procedure have been validated on the four-wheel skid-steer Quadriga mobile robot with four combinations of load and terrain types. Results have shown that this simple model closely resembles measured power consumption in test paths.

Future work includes testing the power model in other terrains, such as asphalt. It would also be interesting to extend the model so as to incorporate the effect of wheel passive suspension on irregular terrain. Moreover, an automatic online implementation of the identification procedure would
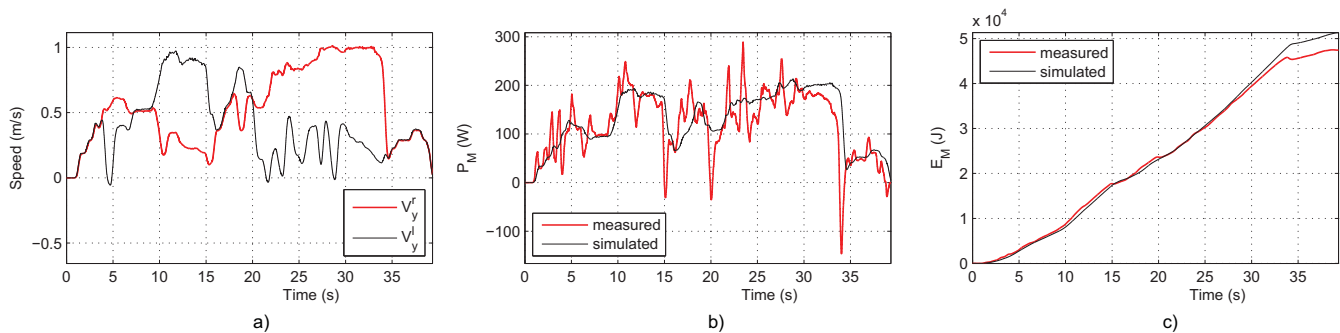
Fig. 6.   Validation path on marble flooring with empty tank: a) Wheel speeds, b) Simulated and measured instantaneous mechanical power, and c) Integral of simulated and measured power.
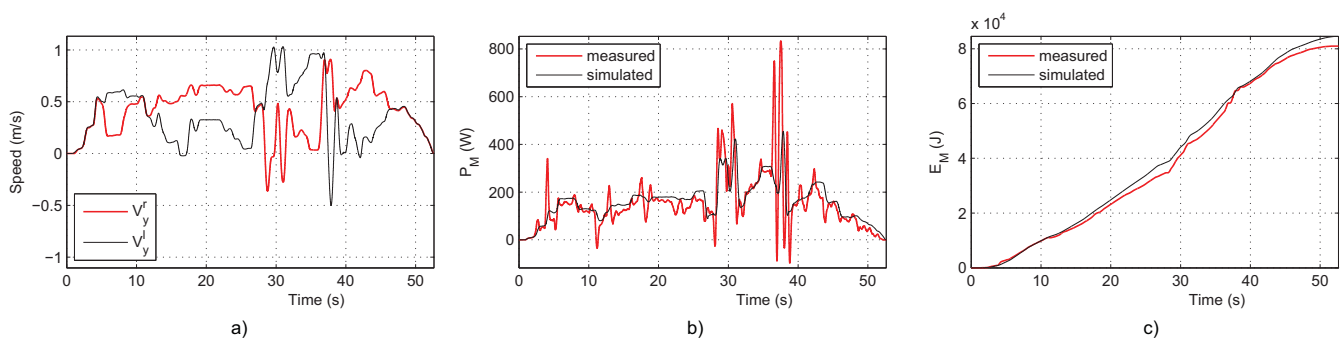
Fig. 7.   Validation path on marble flooring with full tank: a) Wheel speeds, b) Simulated and measured instantaneous mechanical power, and c) Integral of simulated and measured power.
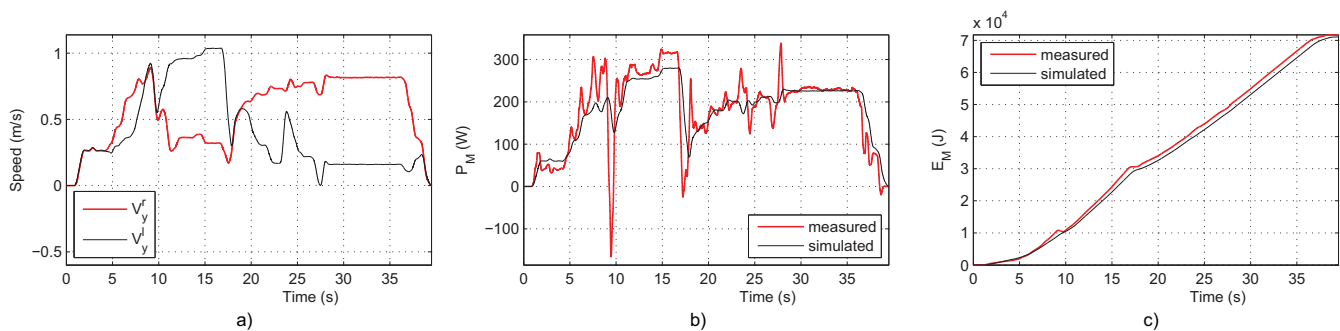
Fig. 8.   Validation path on concrete with empty tank: a) Wheel speeds, b) Simulated and measured instantaneous mechanical power, and c) Integral of simulated and measured power.
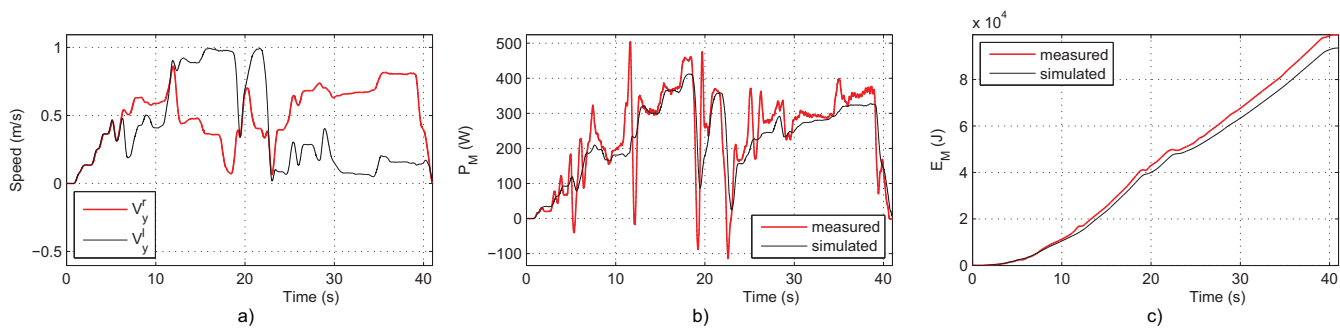
Fig. 9.   Validation path on concrete with full tank: a) Wheel speeds, b) Simulated and measured instantaneous mechanical power, and c) Integral of simulated and measured power.

be valuable to recalculate model parameters in missions where terrain type is unknown.

REFERENCES

[1] B. Shamah, M. D. Wagner, S. Moorehead, J. Teza, D. Wettergreen, and W. Whittaker, "Steering and control of a passively articulated robot," in *SPIE Sensor Fusion and Decentralized Control in Robotics Systems IV*, 2001.

[2] D. E. Pebrian and A. Yahya, "Comparisons on engine power requirements of 6WD and 4WD prime movers for the oil palm plantation in Malaysia," *Journal of Terramechanics*, vol. 47, pp. 131–142, 2010.

[3] J. Y. Wong and W. Huang, "Wheels vs. tracks: A fundamental evaluation from the traction perspective," *Journal of Terramechanics*, vol. 43, pp. 27–42, 2006.

[4] B. Maclaurin, "Comparing the steering performances of skid- and Ackermann-steered vehicles," *Proc. of the Institution of Mechanical Engineers, Part D: Journal of Automobile Engineering*, vol. 222, no. 5, pp. 739–756, 2008.

[5] J. Yi, H. Wang, J. Zhang, D. Song, S. Jayasuriya, and J. Liu, "Kinematic modeling and analysis of skid-steered mobile robots with applications to low-cost inertial-measurement-unit-based motion estimation," *IEEE Transactions on Robotics*, vol. 25, no. 5, pp. 1087–1097, 2009.

[6] L. Zalud, L. Kopecny, and F. Burian, "Orpheus reconnissance robots," in *Proc. of the IEEE International Workshop on Safety, Security and Rescue Robotics*, Sendai, Japan, 2008, pp. 31–34.

[7] A. Chetchetka, S. Hughes, R. Glinton, M. Koes, M. Lewis, I. Nourbakhsh, D. Rosenberg, K. Sycara, and J. Wang, "Robocup rescue robot league team raptor (USA)," in *Proc. RoboCup US Open 2005 Rescue Robot League Competition*, Atlanta, Georgia, USA, 2005.

[8] R. Ray, B. Bepari, and S. Bhaumik, *Intelligent Autonomous Systems*. Springer-Verlag, 2010, ch. 5: "On Design and Development of an Intelligent Mobile Robotic Vehicle for Stair-Case Navigation", pp. 87–122.

[9] J. C. Fauroux and P. Vaslin, "Modeling, experimenting, and improving skid steering on a 6x6 all-terrain mobile platform," *Journal of Field Robotics*, vol. 27, no. 2, pp. 107–126, 2010.

[10] O. Chuy, E. G. Collins, W. Yu, and C. Ordonez, "Power modeling of a skid steered wheeled robotic ground vehicle," in *Proc. IEEE International Conference on Robotics and Automation*, Kobe, Japan, 2009, pp. 4118–4123.

[11] J. Morales, J. L. Martínez, A. Mandow, A. García-Cerezo, and S. Pedraza, "Power consumption modeling of skid-steer tracked mobile robots on rigid terrain," *IEEE Transactions on Robotics*, vol. 25, no. 5, pp. 1098–1108, 2009.

[12] A. Mandow, J. L. Martínez, J. Morales, J. L. Blanco, A. García-Cerezo, and J. González, "Experimental kinematics for wheeled skid-steer mobile robots," in *Proc. of the IEEE/RSJ International Conference on Intelligent Robots and Systems*, San Diego, U.S.A., 2007, pp. 1222–1227.

[13] J. L. Martínez, A. Mandow, J. Morales, S. Pedraza, and A. García-Cerezo, "Aproximating kinematics for tracked mobile robots," *The International Journal of Robotics Research*, vol. 24, no. 10, pp. 867–878, 2005.

[14] W. Press, S. Teukolsky, W. Vetterling, and B. Flannery, *Numerical Recipes in C*, 2nd ed. Cambridge, UK: Cambridge University Press, 1992.